Short communication

1993-03-02

The Diffuse View Factors between Enclosed Surfaces in a Rotary Kiln Incinerator

Y. Y. CHEN[1]

Department of Chemical Engineering, Yuan-Ze Institute of Technology, Taoyuan, Taiwan 32026, R.O.C.

R. H. CHANG[2]

Energy and Resources Laboratories, Industrial Technology Research Institute, Hsinchu, Taiwan 31015, R.O.C.

D. J. LEE[3]

Department of Chemical Engineering, National Taiwan University, Taipei, Taiwan 10617, R.O.C.

Key Words: Diffuse View Factor, Rotary Kiln Incinerator, Working Equations.

INTRODUCTION

In many high temperature industrial applications, the radiation heat transfer plays a very important role in the heat/mass transfer processes, as in the rotary kiln process (Watkinson and Brimacombe, 1978; Tscheng and Watkinson, 1979; Gorog, *et al.*, 1982; Barr, *et al.*, 1989a, 1989b; Chang, 1990). To estimate the contribution of radiation heat transfer rate between nonisothermal enclosures in such processes, the view factors are the basic information needed in calculation. The diffuse view factors for many simple geometry had been evaluated in literature and were summarized in several books (Ozisik, 1973; Sparrow and Cess, 1978; Siegel and Howell, 1981). However, all the diffuse view factors needed in rotary kiln processes were still lack to the authors' best knowledge.

The basic geometry of a rotary kiln was a circular hollow tube partially filled with a solid bed and was bounded by two side walls. Since the temperature did not distribute uniformly along the solid bed and the tube wall, and since the side walls might also have large contribution on the radiation heat transfer, the diffuse view factors between the solid bed, the refractory wall, and the side walls were needed.

In this note, the diffuse view factors between various enclosed surfaces in a rotary kiln were evaluated by contour integration followed by numerical integration. The results were correlated into several working equations which were simple in form and could be applied easily in further analysis.

ANALYSIS

In the following analysis, the view factors between the surfaces shown in Fig. 1a to 1e would be referred to as Case A to Case E, respectively. $F_{dP_1-A_2}$, the diffuse view factor between an elemental surface dP_1 and the surface A_2 shown in Fig. 2(a), and $F_{dA_3-A_4}$, the diffuse view factor between elemental surface dA_3 and surface A_4 shown in Fig. 2(b), will be needed in further calculations. Therefore, the analytical solutions of these two factors were derived in Appendix I.

In this work, the fill angle $2\theta^\circ$ was taken as a constant along the kiln. It was noted that the view factor between two surfaces will remain unchanged if the surfaces exchange according to their axial positions. Therefore, only the conditions when the position vector between two enclosed surfaces was positive would be disscussed.

1. Case A

Consider the diffuse view factor between dP_1 and A_2 in Fig. 1(a), it was clear that the value could be evaluated by direct integration of as:

$$2R \sin\theta^\circ dz_1 F_{dP_1-A_2} = \int_{dP_1} F_{dA_1-A_2} dy_1 dz_1 \qquad (1)$$

Therefore,

[1] 陳宇仰

[2] 張榮興

[3] 李篤中, To whom all correspondences should be addressed.

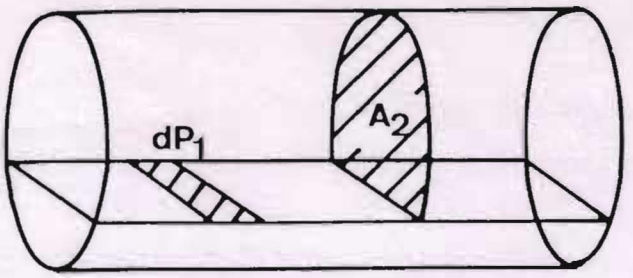

Fig. 1(a). Diffuse view factor between segment dP_1 and surface A_2.

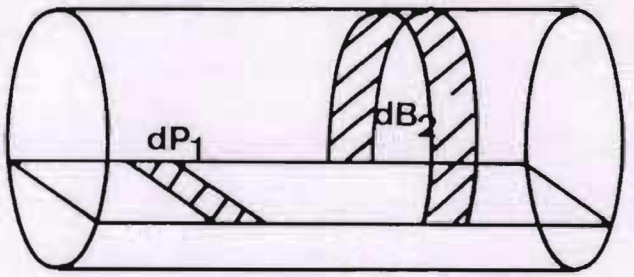

Fig. 1(b). Diffuse view factor between segment dP_1 and band dB_2.

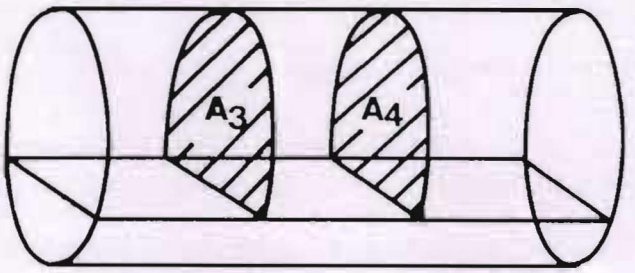

Fig. 1(c). Diffuse view factor between surfaces A_3 and A_4.

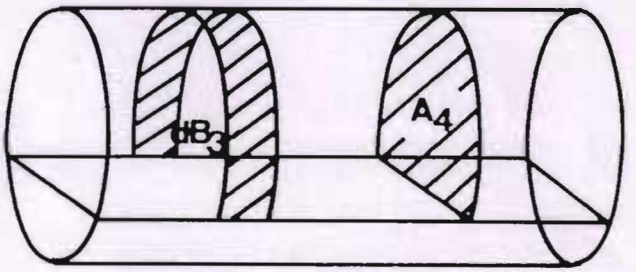

Fig. 1(d). Diffuse view factor between band dB_3 and surface A_4.

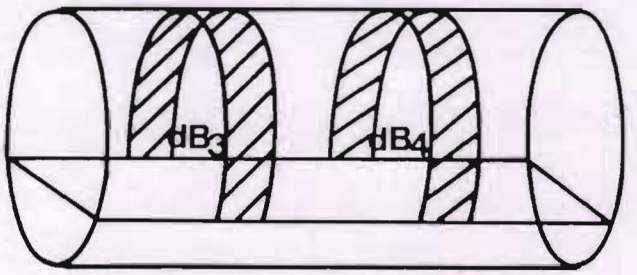

Fig. 1(e). Diffuse view factor between band dB_3 and band dB_4.

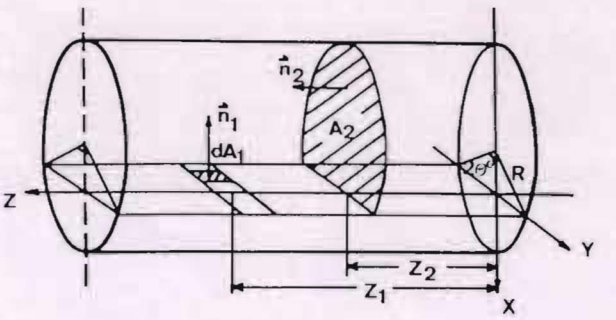

(a)

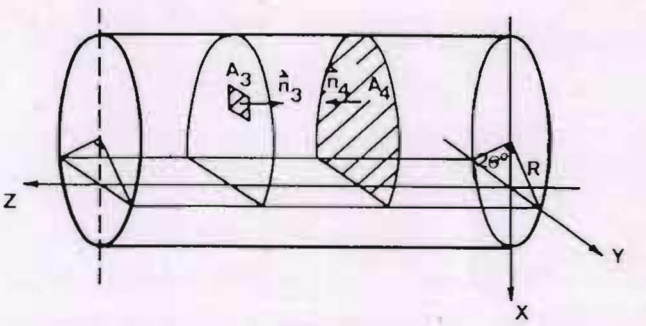

(b)

Fig. 2. Coordinate system employed in this work.

$$F_{dP_1-A_2}=\frac{1}{2R\sin\theta^2}\int_{-R\sin\theta^0}^{R\sin\theta^0}F_{dA_1-A_2}dy_1$$
$$=\frac{1}{2\sin\theta^0}\int_{-\sin\theta^0}^{\sin\theta^0}F_{dA_1-A_2}dy_1^+ \qquad (2)$$

where $y_1^+=y_1/R$.

Since there existed no analytical solution of Eq. (2), numerical integration was needed.

2. Case B

The view factor between dP_1 to the band surface dB_2 shown in Fig. 1(b) could be obtained as:

$$dF_{dP_1-dB_2}=F_{dP_1-A_2|Z_2+dZ_2}-F_{dP_1-A_2|Z_2}$$
$$=\frac{\partial}{\partial Z_2}(F_{dP_1-A_2})dZ_2 \qquad (3)$$

Substitute Eq. (2) into Eq. (3), the result was:

$$dF_{dP_1-dB_2}$$
$$=\frac{1}{2R\sin\theta^0}\frac{d}{dZ_0}\left(\int_{-R\sin\theta^0}^{R\sin\theta^0}F_{dA_1-A_2}dy_1\right)dZ_0 \qquad (4)$$

The following relation held:

$$\frac{d}{dZ_0}\left(\int_{-R\sin\theta^0}^{R\sin\theta^0}F_{dA_1-A_2}dy_1\right)$$
$$=\int_{-R\sin\theta^0}^{R\sin\theta^0}\left(\frac{\partial}{\partial Z_0}F_{dA_1-A_2}\right)dy_1 \qquad (5)$$

Thus, Eq. (4) became:

$$dF_{dP_1-dB_2} = \frac{1}{2\sin\theta^0}\int_{-\sin\theta^0}^{\sin\theta^0}\frac{\partial}{\partial Z_0^+}(F_{dA_1-A_2})dy_1^+dZ_0^+ \quad (6)$$

The differentiation of $F_{dA_1-A_2}$ with respect to Z_0^+ in Eq. (6) could be shown analytically as follows:

$$\frac{\partial}{\partial Z_0^+}F_{dA_1-A_2} = -\frac{1}{2\pi}[Y_a+Y_b-Y_c(\pi+Y_d-Y_e)+Y_f(Y_g-Y_h)] - \frac{Z_0^+}{2\pi}[Y_{a1}-Y_{c1}(\pi+Y_d-Y_e)-Y_c(Y_{d1}-Y_{e1}) + Y_{f1}(Y_g-Y_h)+Y_f(Y_{g1}-Y_{h1})] \quad (7)$$

where

$$Y_{a1}=\frac{c}{b^2+c^2}\frac{4Z_0^+c\sin\theta^0}{(a+b\cos\theta^0-c\sin\theta^0)(a+b\cos\theta^0+c\sin\theta^0)} \quad (8a)$$

$$Y_{c1}=-\frac{4bZ_0^+}{(a^2-b^2-c^2)^{3/2}} \quad (8b)$$

$$Y_{d1}=\frac{-2Z_0^+\tan\left(\frac{\theta^0}{2}\right)(a^2-b^2-c^2)-2aZ_0^+\left[-(a-b)\tan\left(\frac{\theta^0}{2}\right)+c\right]}{\left\{a^2-b^2-c^2+\left[-(a-b)\tan\left(\frac{\theta^2}{2}\right)+c\right]^2\right\}\sqrt{a^2-b^2-c^2}} \quad (8c)$$

$$Y_{e1}=\frac{2Z_0^+\tan\left(\frac{\theta^0}{2}\right)(a^2-b^2-c^2)-2aZ_0^+\left[(a-b)\tan\left(\frac{\theta^0}{2}\right)+c\right]}{\left\{a^2-b^2-c^2+\left[(a-b)\tan\left(\frac{\theta^0}{2}\right)+c\right]^2\right\}\sqrt{a^2-b^2-c^2}} \quad (8d)$$

$$Y_{f1}=\frac{(b_1-a_1)Z_0^+\cos\theta^0}{(a_1^2-b_1^2-c_1^2)^{3/2}} \quad (8e)$$

$$Y_{g1}=\frac{(b_1-a_1)Z_0^+\left[\frac{(\sin\theta^0)}{2}+c_1\right]}{\left\{a_1^2-b_1^2-c_1^2+\left[\frac{(\sin\theta^0)}{2}+c_1\right]^2\right\}\sqrt{a_1^2-b_1^2-c_1^2}} \quad (8f)$$

$$Y_{h1}=\frac{(b_1-a_1)Z_0^+\left[-\frac{(\sin\theta^0)}{2}+c_1\right]}{\left\{a_1^2-b_1^2-c_1^2+\left[-\frac{(\sin\theta^0)}{2}+c_1\right]^2\right\}\sqrt{a_1^2-b_1^2-c_1^2}} \quad (8g)$$

Numerical integration was also needed to evaluate the integration term in Eq. (6).

3. Case C

The diffuse view factor between dA_3 and A_4 in Fig. 1(c) was shown in Eq. (A-8). Therefore, the diffuse view factor from A_3 to A_4 could be found from surface integration as:

$$F_{A_3-A_4}=\frac{1}{A_3}\iint_{A_3}F_{dA_3-A_4}dA_3 \quad (9)$$

Numerical double integration was required in this case.

4. Case D

From point of conservation of energy, the following equation held for the view factors shown in Fig. (1d):

$$F_{A_4-dB_3}+F_{A_4-dP_3}=\frac{\partial}{\partial Z_3}F_{A_4-A_3} \quad (10)$$

From Eqs. (2), (9), and (10), the following result could be obtained by applying Leibniz's rule:

$$F_{dB_3-A_4}=\frac{1}{2R(\pi-\theta^0)}\iint_{A_4}\frac{\partial}{\partial Z_0}F_{dA_4-A_3}rdrd\theta - \frac{\sin\theta^0}{\pi-\theta^0}F_{dP_3-A_4} \quad (11)$$

In Eq. (11), the last term could be found from Eq. (2) and the differentiation term could be shown analytically as

$$\frac{\partial}{\partial Z_0}F_{dA_4-A_3} = -\frac{1}{2\pi}[Z_{c1}(\pi+Z_d-Z_e)+Z_c(Z_{d1}-Z_{e1})] - \frac{d_3}{4\pi}[Z_{h1}(Z_f-Z_g)+Z_h(Z_{f1}-Z_{g1})] \quad (12)$$

where

$$Z_{c1}=\frac{2Z_0^+[a^2-b^2-c^2-a(r_1^{+2}+Z_0^{+2}-1)]}{(a^2-b^2-c^2)^{3/2}} \tag{13a}$$

$$Z_{d1}=-2Z_0^+\left\{\frac{\tan\left(\frac{\theta^0}{2}\right)(a^2-b^2-c^2)+a\left[-(a-b)\tan\left(\frac{\theta^0}{2}\right)+c\right]}{\sqrt{a^2-b^2-c^2}\left\{a^2-b^2-c^2+\left[-(a-b)\tan\left(\frac{\theta^2}{2}\right)+c\right]^2\right\}}\right\} \tag{13b}$$

$$Z_{e1}=2Z_0^+\left\{\frac{\tan\left(\frac{\theta^0}{2}\right)(a^2-b^2-c^2)-a\left[(a-b)\tan\left(\frac{\theta^0}{2}\right)+c\right]}{\sqrt{a^2-b^2-c^2}\left\{a^2-b^2-c^2+\left[(a-b)\tan\left(\frac{\theta^0}{2}\right)+c\right]^2\right\}}\right\} \tag{13c}$$

$$Z_{f1}=\frac{-Z_0^+(a_3-b_3)\left[\frac{(\sin 2\theta^0)}{2}+c_3\right]}{\sqrt{a_3^2-b_3^2-c_3^2}\left\{a_3^2-b_3^2-c_3^2+\left[\frac{(\sin 2\theta^0)}{2}+c_3\right]^2\right\}} \tag{13d}$$

$$Z_{g1}=\frac{-Z_0^+(a_3-b_3)\left[-\frac{(\sin 2\theta^0)}{2}+c_3\right]}{\sqrt{a_3^2-b_3^2-c_3^2}\left\{a_3^2-b_3^2-c_3^2+\left[-\frac{\sin(2\theta^0)}{2}+c_3\right]^2\right\}} \tag{13e}$$

$$Z_{h1}=\frac{-2Z_0^+(a_3-b_3)}{(a_3^2-b_3^2-c_3^2)^{3/2}} \tag{13f}$$

Numerical integration was also needed to evaluate the double integration in Eq. (11).

5. Case E

From the law of the conservation of energy, the following equation held:

$$dF_{dB_3-dB_4}+dF_{dP_3-dB_4}=\frac{\partial}{\partial Z_4}(F_{dB_3-A_4})dZ_4 \tag{14}$$

Substitute Eq. (11) into Eq. (14) we can get

$$\begin{aligned}dF_{dB_3-dB_4}&=\frac{\partial}{\partial Z_4}(F_{dB_3-A_4})dZ_4-dF_{dB_3-dP_4}\\&=\frac{1}{2R(\pi-\theta^0)}\left(\iint_{A_4}\frac{\partial^2}{\partial Z_0^2}F_{dA_4-A_3}rdrd\theta\right)\cdot dZ_0\\&\quad-\frac{2\sin\theta^0}{\pi-\theta^0}dF_{dP_4-dB_3}\end{aligned} \tag{15}$$

To evaluate Eq. (15), double integration of the second order differentiation of $F_{dA_4-A_3}$ was needed. But it was found in the latter calculations that the direct integration of the second order differentiation form was numerically undesirable, since the integration became very stiff when $|Z_0^+|$ approached zero. Therefore, the first order differentiation form Eq. (12) was integrated first, and then numerical differentiation was applied to evaluate the required value in Eq. (15).

NUMERICAL METHODS

The view factors $F_{dP_1-A_2}$, $dF_{dP_1-dB_2}$, $F_{A_3-A_4}$, $F_{dB_3-A_4}$, and $dF_{dB_3-dB_4}$ would be obtained if Eqs. (2), (6), (9), (11), and (15) could be evaluated. Since no analytical solutions of these equations were available, numerical solutions were needed.

To perform the single integration in this work (Eqs. (2) and (6)), Gear's method was directly applied. The relative errors were all controlled to be under 10^{-6}. For the double integration calculations (Eqs. (9), (11) and (15)), the inner shell of integration (the r domain) were evaluated by Gear's method, and the outer shell of integration (the θ domain) were divided into 2^N panels and each panel was calculated by six-point Gaussian quadrature. To check the convergence of the integrations, the results from 2^N panels were compared with the integral values form the 2^{N+1} panels. If the result was not converged, each panel is divided into two sub panels, and the procedure was repeated. The tolerance used in double integrations was 10^{-6}. Usually, the N value needed for satisfactory integration was about 6 to 7.

To evaluate Eq. (15), central difference scheme was used in numerical differentiation calculations.

RESULTS AND DISCUSSIONS

General

The view factors evaluated from Eqs. (2), (6), (9), (11) and (15) with θ^0 as the parameter when shown in Figs. 3 to 7. It was clear that the view factors all decreased as Z_0^+ increased and would approach to zero when $Z_0^+ \to \infty$. It was also clear that the view factors would decrease to below 0.05 when $|Z_S^+|$ was larger than about 3.0. Therefore, for a long rotary kiln, the enclosed surfaces which were three radius away from the surface could be neglected in practice.

The effects of θ^0 on $F_{dP_1-A_2}$, $F_{A_3-A_4}$, and $F_{dB_3-A_4}$, were minor when compared with the effects of Z_0^+, which suggested that these view factors could also be used in the applications whose θ^0 changed continuously along the tube.

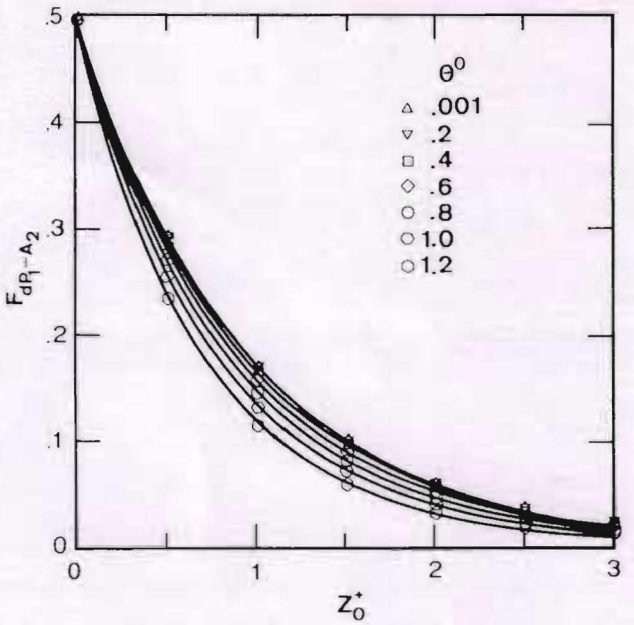

Fig. 3. Diffuse view factor $F_{dP_1-A_2}$ *vs.* Z_0^+. The correlation equation (Eq. (21)) was shown as solid lines for comparisons.

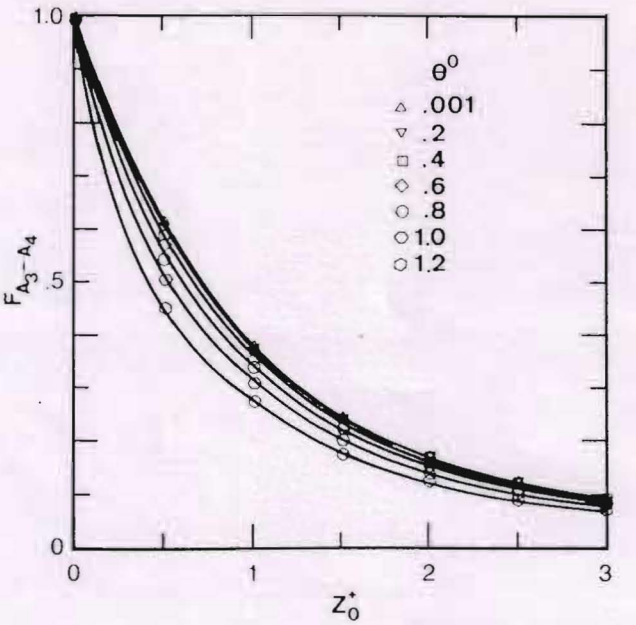

Fig. 5. Diffuse view factor $F_{A_3-A_4}$ *vs.* Z_0^+. The correlation equation (Eq. (23)) was shown as solid lines for comparisons.

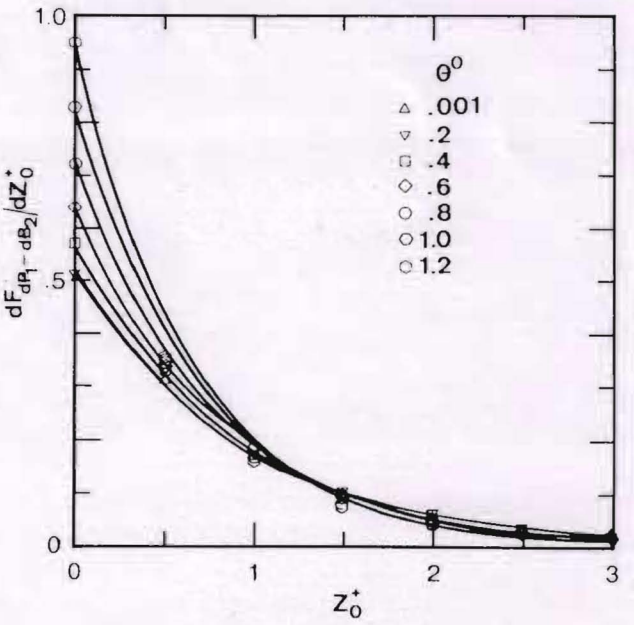

Fig. 4. Diffuse view factor $dF_{dP_1-dB_2}$ *vs.* Z_0^+. The correlation equation (Eq. (22)) was shown as solid lines for comparisons.

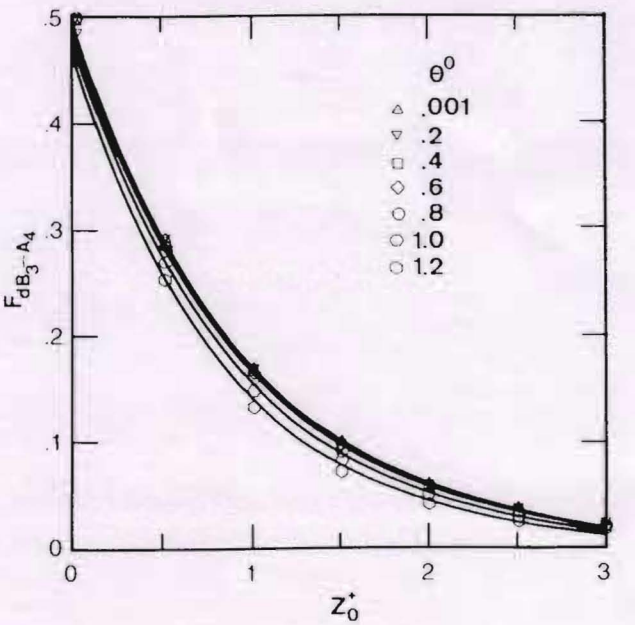

Fig. 6. Diffuse view factor $F_{dB_3-A_4}$ *vs.* Z_0^+. The correlation equation (Eq. (24)) was shown as solid lines for comparisons.

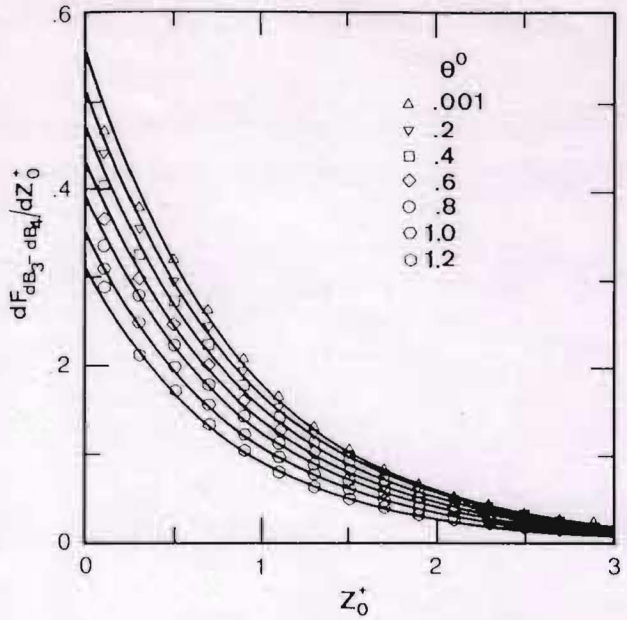

Fig. 7. Diffuse view factor $dF_{dB_3-dB_4}$ *vs.* Z_0^+. The correlation equation (Eq. (25)) was shown as solid lines for comparisons.

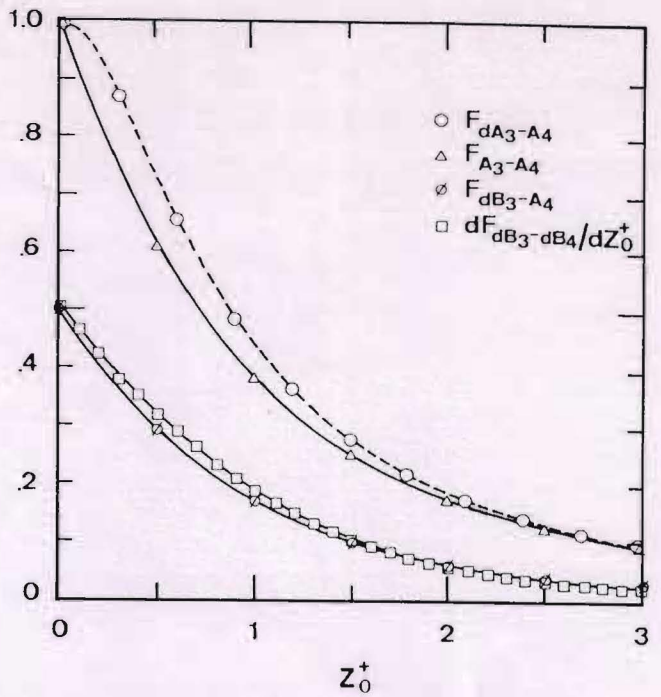

Fig. 8. The comparisons between numerical results with analytical solution found in Ozisik (1973) (solid lines) and in Sparrow and Cess (1978) (dashed line).

Though there existed no analytical and/or numerical results in literature with which our calculation results could be compared, several physical interpretations were used to check the accuracy of the current work. First, when the segment dP_1 and surface A_2 in Fig. 1(a) approached to each other, the view factor from dP_1 to A_2 should approach 0.5, *i.e.*,

$$\lim_{z_0^+ \to 0} F_{dP_1-A_2}=0.5 \tag{16}$$

Similarly,

$$\lim_{z_0^+ \to 0} F_{dB_1-A_2}=0.5 \tag{17}$$

and

$$\lim_{z_0^+ \to 0} F_{A_3-A_4}=1.0 \tag{18}$$

These properties were clearly shown in Figs. 3, 5, and 6.

Second, when $\theta^\circ \to 0$, $F_{dA_3-A_4}$, became the view factor from elemental surface to a circular disk which could be found in Sparrow and Cess (1980) and $dF_{dB_3-dB_4}$, should be the same as the view factor between two elemental coaxial circular bands which was also listed in Ozisik (1973). Figure 8 showed the numerical results of Eqs. (9) and (15) ($\theta^\circ=0.001$) and the analytical solutions (the lines). It was clear that the numerical results coincided with the analytical solutions.

Third, when a segment dP_1 was placed at the edge of a semi-infinite tube (as shown in Fig. 9),

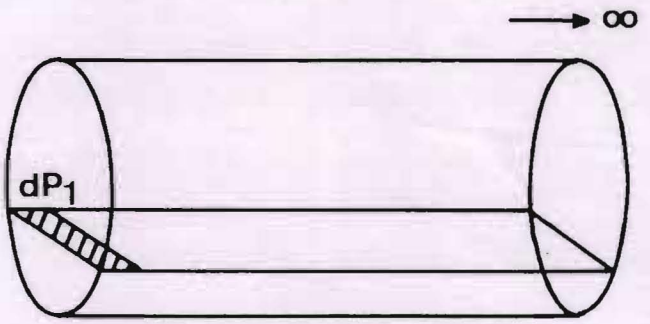

Fig. 9. The diffuse view factor from segment dP_1 to a semi-infinite tube wall.

half of the radiative energy leaving dP_1 would be captured by the tube wall, *i.e.*,

$$I_1=\int_{Z_0^+=0}^{Z_0^+=\infty} dF_{dP_1-dB_2}=0.5 \tag{19}$$

For the same reason, the following relation also held:

$$I_2=\int_{Z_0^+=0}^{Z_0^+=\infty} dF_{dB_3-dB_4}+dF_{dB_3-dP_4}=0.5 \tag{20}$$

The calculated view factors were then integrated by Simpson's rule and the results were shown in Figs. 10(a) and 10(b). It was clear that Eqs. (19) and (20) held with errors less than 1% when $|Z_0^+|$ was larger than about 6.0.

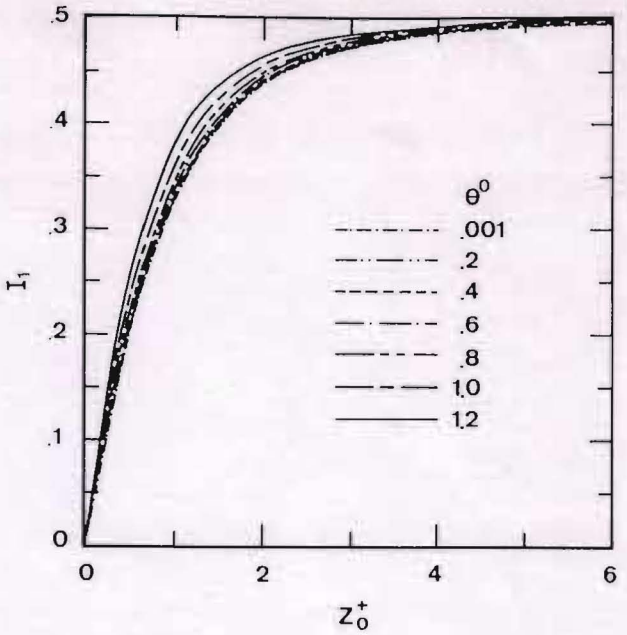

(a)

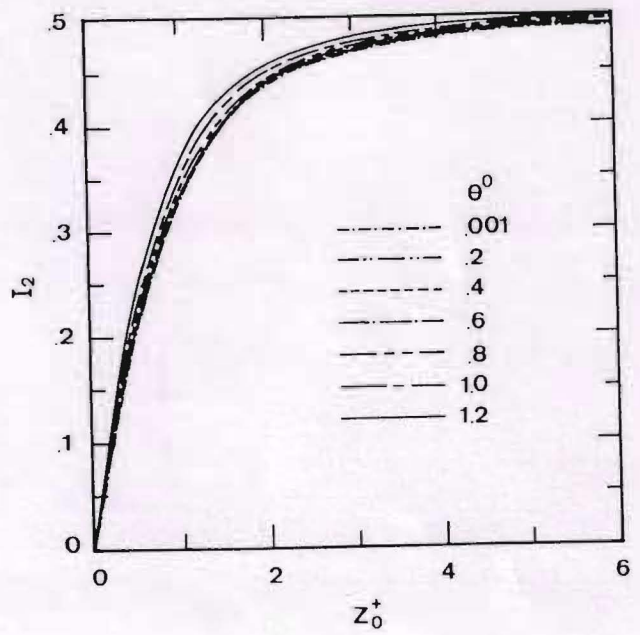

(b)

Fig. 10. The integration test of (a) Eq. (19) and (b) Eq. (20). It was clear that when $|Z_0^+|$ was larger than about 6.0, Eqs. (19) and (20) could be satisfied for all θ° studied.

From the above discussions, it was believed that the current results were accurate enough for most applications.

Working equations

For the sake of convenience for further usage, the view factors evaluated numerically were correlated as simple functional form as the working equations. The results for Case A to Case E were listed as follows.

1. Case A

$$F_{dP_1-A_2}=\sum_{i=1}^{4}\alpha_i|Z_0^+|^i \tag{21a}$$

where

$$\alpha_i=\sum_{j=0}^{3}\alpha_i^j\theta^{\circ j} \tag{21b}$$

2. Case B

$$dF_{dP_1-dB_2}=\sum_{i=0}^{5}\beta_i|Z_0^+|^i dZ_0^+ \tag{22a}$$

where

$$\beta_i=\sum_{j=0}^{3}\beta_i^j\theta^{\circ j} \tag{22b}$$

3. Case C

$$F_{A_3-A_4}=F_0(\tau_0+\tau_1\theta^\circ+\tau_2\theta^{\circ 2}) \tag{23a}$$

where

$$F_0=\sum_{i=0}^{6}\sigma_i|Z_0^+|^i \tag{23b}$$

4. Case D

$$F_{dB_3-A_4}=\sum_{i=0}^{4}\delta_i|Z_0^+|^i \tag{24a}$$

where

$$\delta_i=\sum_{j=0}^{3}\delta_i^j\theta^{\circ j} \tag{24b}$$

The coefficients α_i^j, β_i^j, τ_i, σ_i, and δ_i^j were all listed in Appendix II.

5. Case E

$$dF_{dB_3-dB_4}=M\exp(N|Z_0^+|)dZ_0^+ \tag{25}$$

where

$$M=-0.2031\theta^\circ+0.5529 \tag{25b}$$

$$N=-0.21716(1-\cos\theta^\circ)^2 \tag{25c}$$

The working equations Eqs. (21) to (25) were also shown as solid lines in Figs. 3 to 7. It was shown that for most cases, the averaged relative errors would be within 2%. These equations were valid within $|Z_0^+|\leq 3$. When $|Z_0^+|$ was larger than 3, the view factors could be taken as zero in practice.

CONCLUSIONS

The diffuse view factors between enclosed surfaces in a rotary kiln were evaluated by contour integration followed by numerical integration. The accuracy of the calculations were checked by several physical interpretations. The results were correlated into several working equations which were simple in form and could be applied in further analysis.

ACKNOWLEDGEMENTS

This work was supported by Energy and Resources Laboratories, Industrial Technology Research Institute, Hsinchu, Taiwan, R.O.C.

NOMENCLATURE

A	area, (m^2)
F	diffuse view factor, $(-)$
I_1, I_2	integrations defined in Eqs. (19) and (20)
R	kiln radius, (m)
r	distance, (m)
y_1, y_2	positions at y direction, (m)
Z_0^+	$=(z_2-z_1)/R$
z_1, z_2, z_3, z_4	positions at z direction, (m)

Greek Letter

θ^0	half of the fill angle, (rad)

REFERENCES

Barr, P.V., J.K. Brimacombe and A.P. Watkinson, "Heat-Transfer Model for the Rotary Kiln: Part I. Pilot Kiln Trials", *Metall. Trans. B.*, **20B**, 391 (1989a).

Barr, P.V., J.K. Brimacombe and A.P. Watkinson, "Heat-Transfer Model for the Rotary Kiln: Part II. Development of the Cross-Section Model", *Metall. Trans. B.*, **20B**, 403 (1989b).

Chang, R.H., "Heat and Mass Transfer in a Rotary Kiln Incinerator", *Proc. Symp. Transport Phenomena and Applications*, Taipei (1990).

Gorog, J.P., T.N. Adams and J.K. Brimacombe, "Regenerative Heat Transfer in Rotary Kilns", *Metall. Trans. B.*, **13B**, 153 (1982).

Ozisik, M.N., *Radiative Transfer*, John Wiley and Sons, New York (1973).

Sparrow, E.M. and R.D. Cess, *Radiation Heat Transfer*, Hemisphere Pub., Washington DC (1978).

Siegel, R. and J.R. Howell, *Thermal Radiation Heat Transfer*, McGraw-Hill, New York (1981).

Tscheng, S.H. and A.P. Watkinson, "Convective Heat Transfer in a Rotary Kiln" *Can. J. Chem. Eng.*, **57**, 433 (1979).

Watkinson, A.P. and J.K. Brimacombe, "Heat Transfer in a Direct-Fired Rotary Kiln: II Heat Flow Results and Their Interpretation", *Metall. Trans. B.*, **14B**, 209 (1978).

APPENDIX I

Consider two elemental surfaces dA_1 and dA_2 with uniform temperatures and the normal vector were $\bar{n}_1$ and $\bar{n}_2$ respectively. The diffuse view factor between surfaces dA_1 and dA_2 was defined as:

$$dF_{dA_1-dA_2}=\frac{\cos\theta_1\cos\theta_2 dA_2}{\pi r^2} \tag{A-1}$$

The view factor from dA_1 to a finite surface A_2 can be determined by integrating $dF_{dA_1-dA_2}$ over surface A_2 as

$$F_{dA_1-A_2}=\int_{A_2} dF_{dA_1-dA_2}=\int_{A_2}\frac{\cos\theta_1\cos\theta_2}{\pi r^2}dA_2 \tag{A-2}$$

The evaluation of view factors in equations (A-1) and (A-2) can be performed by applying the stokes theorem to reduce the surface integral to contour integral as in Ozisik (1973).

In the following derivations, the diffuse view factors $F_{dA_1-A_2}$ and $F_{dA_2-A_1}$ needed in further analysis were evaluated analytically as follows.

1. $F_{dA_1-A_2}$ in Fig. 2(a)

For the two surfaces dA_1 and A_2 shown in Fig. 2(a), the diffuse view factor could be represented as:

$$F_{dA_1-A_2}=\frac{-1}{2\pi}\oint_{A_2}\frac{(z_2-z_1)dy_2}{(x_2-x_1)^2+(y_2-y_1)^2+(z_2-z_1)^2} \tag{A-3}$$

Change the coordinate into cylindrical coordinate and integrated analytically, the result was

$$F_{dA_1-A_2}=\frac{-Z_0^+}{2\pi}[Y_a+Y_b-Y_c(\pi+Y_d-Y_e)+Y_f(Y_g-Y_h)] \tag{A-4}$$

where

$$r_1^+=\frac{r_1}{R} \tag{A-5a}$$

$$Z_0^+=\frac{Z_0}{R}=\frac{z_2-z_1}{R} \tag{A-5b}$$

$$Y_a=\frac{c}{b^2+c^2}\ln\left(\frac{a+b\cos\theta^0-c\sin\theta^0}{a+b\cos\theta^0+c\sin\theta^0}\right) \tag{A-5c}$$

$$Y_b=\frac{2b(\pi-\theta^0)}{b^2+c^2} \tag{A-5d}$$

$$Y_c=\frac{ab}{b^2+c^2}\frac{2}{\sqrt{a^2-b^2-c^2}} \tag{A-5e}$$

$$Y_d=\tan^{-1}\left[\frac{-(a-b)\tan\left(\frac{\theta^2}{2}\right)+c}{\sqrt{a^2-b^2-c^2}}\right] \tag{A-5f}$$

$$Y_e=\tan^{-1}\left[\frac{(a-b)\tan\left(\frac{\theta^0}{2}\right)+c}{\sqrt{a^2-b^2-c^2}}\right] \tag{A-5g}$$

$$Y_f=\frac{\cos\theta^0}{\sqrt{a_1^2-b_1^2-c_1^2}} \tag{A-5h}$$

$$Y_g=\tan^{-1}\left[\frac{\frac{(\sin 2\theta^0)}{2}+c_1}{\sqrt{a_1^2-b_1^2-c_1^2}}\right] \tag{A-5i}$$

$$Y_h=\tan^{-1}\left[\frac{-\frac{(\sin 2\theta^0)}{2}+c_1}{\sqrt{a_1^2-b_1^2-c_1^2}}\right] \tag{A-5j}$$

$$a=1+r_1^{+2}+Z_0^{+2} \tag{A-5k}$$

$$b=-2r_1^+\cos\theta_1 \tag{A-5l}$$

$$c=-2r_1^+\sin\theta_1 \tag{A-5m}$$

$$a_1=\cos^2\theta^0+\frac{1}{2}(r_1^{+2}+Z_0^{+2}-2r_1^+\cos\theta^0\cos\theta_1) \tag{A-5n}$$

$$b_1=\frac{1}{2}(r_1^{+2}+Z_0^{+2}-2r_1^+\cos\theta^0\cos\theta_1) \tag{A-5o}$$

$$c_1=-r_1^+\cos\theta^0\sin\theta_1 \tag{A-5p}$$

2. $F_{dA_3-A_4}$ in Fig. 2(b)

The diffuse view factor $F_{dA_3-A_4}$ between surface dA_3 to A_4 shown in Fig. 2(b) was

$$F_{dA_3-A_4}=\frac{1}{2\pi}\oint_{A_4}\frac{(y_4-y_3)dx_4-(x_4-x_3)dy_4}{(x_4-x_3)^2+(y_4-y_3)^2+(z_4-z_3)^2} \tag{A-6}$$

Change the coordinate into cylindrical coordinate and integrated analytically, the result was:

$$F_{dA_3-A_4}=-\frac{1}{2\pi}[Z_b+Z_c(\pi+Z_d-Z_e)]-\frac{d_3}{4\pi}(Z_f-Z_g)Z_h \tag{A-7}$$

where

$$Z_b=\theta^0-\pi \tag{A-8a}$$

$$Z_c=\frac{r_1^{+2}+Z_0^{+2}-1}{\sqrt{a^2-b^2-c^2}} \tag{A-8b}$$

$$Z_d=\tan^{-1}\left[\frac{-(a-b)\tan\left(\frac{\theta^0}{2}\right)+c}{\sqrt{a^2-b^2-c^2}}\right] \tag{4-8c}$$

$$Z_e=\tan^{-1}\left[\frac{(a-b)\tan\left(\frac{\theta^0}{2}\right)+c}{\sqrt{a^2-b^2-c^2}}\right] \tag{A-8d}$$

$$Z_f=\tan^{-1}\left[\frac{\frac{(\sin 2\theta^0)}{2}+c_3}{\sqrt{a_3^2-b_3^2-c_3^2}}\right] \tag{A-8e}$$

$$Z_g=\tan^{-1}\left[\frac{-\frac{(\sin 2\theta^0)}{2}+c_3}{\sqrt{a_3^2-b_3^2-c_3^2}}\right] \tag{A-8f}$$

$$Z_h=\frac{2}{\sqrt{a_3^2-b_3^2-c_3^2}} \tag{A-8g}$$

$$a_3=\cos^2\theta^0+b_3 \tag{A-8h}$$

$$b_3=\frac{1}{2}(r_1^{+2}+Z_0^{+2}-2\cos\theta^0\cos\theta_1 r_1^+) \tag{A-8i}$$

$$c_3=-\cos\theta^0\sin\theta_1 r_1^+ \tag{A-8j}$$

$$d_3=\cos\theta^0\cos\theta_1 r_1^+-\cos^2\theta^0 \tag{A-8k}$$

Equations (A-4) and (A-7) were the fundamental equations which were used in the text.

APPENDIX II

The coefficients of Eqs. (21) to (25) were shown in this Appendix.

1. Case A

$\alpha_0^0=0.5005$	$\alpha_0^1=-0.0142$	$\alpha_0^2=0.0388$	$\alpha_0^3=-0.0237$
$\alpha_1^0=-0.5121$	$\alpha_1^1=0.0477$	$\alpha_1^2=-0.2289$	$\alpha_1^3=0.0399$
$\alpha_2^0=0.2278$	$\alpha_2^1=-0.0456$	$\alpha_2^2=0.2175$	$\alpha_2^3=-0.0223$
$\alpha_3^0=-0.0494$	$\alpha_3^1=0.0171$	$\alpha_3^2=-0.0794$	$\alpha_3^3=0.0055$
$\alpha_4^0=0.0042$	$\alpha_4^1=-0.0022$	$\alpha_4^2=0.01014$	$\alpha_4^3=-0.0005$

2. Case B

$\beta_0^0=0.5004$	$\beta_0^1=0.0594$	$\beta_0^2=0.3106$	$\beta_0^3=-0.0355$
$\beta_1^0=-0.3810$	$\beta_1^1=-0.2340$	$\beta_1^2=-1.1127$	$\beta_1^3=0.1487$
$\beta_2^0=0.02225$	$\beta_2^1=0.1120$	$\beta_2^2=1.9487$	$\beta_2^3=-0.5206$
$\beta_3^0=0.0728$	$\beta_3^1=0.1014$	$\beta_3^2=-1.6151$	$\beta_3^3=0.5725$
$\beta_4^0=-0.0290$	$\beta_4^1=-0.0781$	$\beta_4^2=0.5876$	$\beta_4^3=-0.2353$
$\beta_5^0=0.00348$	$\beta_5^1=0.01333$	$\beta_5^2=-0.0762$	$\beta_5^3=0.03243$

3. Case C

$\gamma_0=0.9840$ $\gamma_1=0.1228$ $\gamma_2=-0.28306$
$\sigma_0=0.9970$ $\sigma_1=-0.95545$ $\sigma_2=0.4371$ $\sigma_3=-0.1098$
$\sigma_4=0.0153$ $\sigma_5=-0.0011$ $\sigma_6=0.00003$

$\delta_1^0=-0.5189$ $\delta_1^1=-0.00386$ $\delta_1^2=-0.0045$ $\delta_1^3=-0.07459$
$\delta_2^0=0.2338$ $\delta_2^1==0.0042$ $\delta_2^2=0.00645$ $\delta_2^3=0.0804$
$\delta_3^0=-0.05134$ $\delta_3^1=-0.0015$ $\delta_3^2=-0.00347$ $\delta_3^3=-0.0304$
$\delta_4^0=0.00447$ $\delta_4^1=0.00015$ $\delta_4^2=0.00063$ $\delta_4^3=0.0039$

4. Case D

$\delta_0^0=0.5025$ $\delta_0^1=0.00233$ $\delta_0^2=-0.0049$ $\delta_0^3=0.00237$

(Manuscript Received January 19, 1993, Accepted April 29, 1993)

旋窯焚化爐內部各表面間之擴散視因子

陳 宇 仰
私立元智工學院化工系

張 榮 興
工研院能源與資源研究所

李 篤 中
國立臺灣大學化工系

摘 要

一個旋窯焚化爐內部各表面間的輻射熱傳送對其效能有很大的影響。當要估算旋窯內部各不同溫度之表面間的輻射照傳量時，需要先知道旋窯壁、固體床及旋窯兩端窯壁等各表面間的擴散視因子，但這些資料在文獻中部沒有報導。在本文中，我們使用邊界積分及數值積分計算這些視因子，並將所得結果迴歸成數個簡單型式的工作函數，以供未來進一步之應用。

Abstract

Thermal radiation heat transfer between enclosed surfaces in a rotary kiln incinerator is believed to play an important role in determining the system performance but has not been fully investigated. The diffuse view factors between these surface are the basic information for estimating the rediation heat flux but are still lack in literature. In this work, the diffuse view factors between the refractory wall, the solid bed, and the side walls are evaluated by contour integration follows by numerical integration. The results are correlated into several working equations which are simple in form and can be applied in further analysis.